Available online at www.sciencedirect.com
ScienceDirect
BioSystems 86 (2006) 100–109
Bio Systems
www.elsevier.com/locate/biosystems

Neural coding for the retrieval of multiple memory patterns

A. Morelli[a,*], R. Lauro Grotto[b], F.T. Arecchi[c]

[a] *Centro Interdipartimentale per lo Studio di Dinamiche Complesse (CSDC), Department of Physics, University of Florence, Italy*
[b] *Department of Psychology, University of Florence, Italy*
[c] *Department of Physics, University of Florence, Italy*

Received 15 December 2005; received in revised form 23 February 2006; accepted 7 March 2006

Abstract

We investigate the retrieval dynamics in a feature-based semantic memory model, in which the features are coded by neurons of the Hindmarsh–Rose type in the chaotic regime. We consider the retrieval process as consisting of the synchronized firing activity of the neurons coding for the same memory pattern. The retrieval dynamics is investigated for multiple patterns, with particular attention to the case of overlapping memories. In this case, we hypothesize a dynamical *nontransitive* mechanism based on synchronization, that allows for a shared feature to participate in multiple memory representations. The problem of the choice of a cognitive plausible time-scale for the retrieval analysis is investigated by analyzing the information that can be inferred from finite-time analyses. Different types of indicators are proposed in order to evaluate the temporal dynamics of the neurons engaged in the retrieval process. We interpret the simulation results as suggestive of a role for chaotic dynamics in allowing for flexible composition of elementary meaningful units in memory representations.

Keywords: Memory model; Neural coding; Chaotic retrieval dynamics; Multiple and overlapping memories; Finite-time analysis

1. Introduction

Memory processes and their neural correlates have been extensively modeled in terms of attractor neural networks (Amit, 1998). Even though these networks provide an effective description of memory retrieval, and recent approaches emphasize the role that dynamic "latching" of attractors might have in unleashing the computational capabilities of fixed point dynamics (Treves, 2005), simultaneous retrieval of overlapping patterns still remains difficult to implement. The problem of memories with a high degree of 'feature ambiguity' has been investigated computationally (Plaut, 1995; Rumelhart, 1990) and experimentally in order to evaluate a possible functional role of the perirhinal cortex in discrimination tasks (Bussey et al., 2003). Here, we focus on this computational problem, namely, the simultaneous retrieval of multiple memory patterns, either overlapping or not. Building on some ideas first proposed for perceptual features (Von der Malsburg, 1999; Engel et al., 1992; Gray, 1999), we explore the possibility to resort to chaotic dynamics in order to implement a semantic memory model in which shared features can be allocated to different dynamic patterns in order to allow for the co-occurring retrieval of two or more related patterns. We indeed have in mind the memorization and retrieval of complex scenes or concepts. Our approach is in agreement with recent studies emphasizing the need to shift towards dynamical paradigms in which memory representations are built 'on the fly' according to the specificity of the task demands and of the behavioral goals the subject is engaged in Shallice (2002). Taking as

* Corresponding author.
E-mail address: morelli@inoa.it (A. Morelli).

0303-2647/$ – see front matter © 2006 Elsevier Ireland Ltd. All rights reserved.
doi:10.1016/j.biosystems.2006.03.011

a starting point the model implemented by Raffone and Van Leeuwen (2003), we study a similar model by implementing a multimodular network in which the features are represented by neurons of the Hindmarsh–Rose type in the chaotic regime. We perform a detailed quantitative analysis of the network behavior by applying different types of synchronicity indicators to the neurons coding for the retrieved memory patterns. First, the memory patterns are investigated by correlation and coincidence analyses over long time intervals. Once long time intervals have been explored, we must consider their limited cognitive plausibility. Taking into account the cognitive time scale over which we perform a decision (e.g. a category judgment), we investigate the neural dynamics over more plausible time windows by a finite-time analysis.

2. Theoretical assumptions and computational problems

We model semantic memory representations with shared features utilizing the following assumptions. First, we assume that a semantic feature is encoded in the collective activity of a segregated population of neurons, thus, the representation is a pattern of activation. For the sake of computational simplicity, we choose to substitute the population dynamics at the featural level with single unit dynamics. Although this is clearly a limit of the present simulations it is nevertheless known that single neuron spiking activity shares many relevant properties with population activity in terms of temporal statistics (Segev et al., 2002). We also assume that neurons coding for features belonging to the same memory pattern synchronize their activity, and neurons coding for features belonging to different patterns do not. Own main concern is the simultaneous retrieval of correlated patterns. This problem could be considered as a version of the well-known *binding problem* in the memory domain. Let us consider the memory retrieval of two simple memory patterns, *apple* and *cherry*, sharing one feature (*reddish*). A possible neuronal mechanism to retrieve simultaneously the two patterns could be to associate two neuronal groups with the shared feature, one synchronized with neurons coding for features belonging to *apple* only, and the other synchronized with neurons belonging to *cherry* only. Since the number of groups increases with the number of patterns to be retrieved, this strategy seems anti-economic. In order to avoid the explosion of the number of groups, we assume that neurons coding for shared features synchronize their activity with the neurons coding for a pattern only, in a *nontransitive* manner (Raffone and Van Leeuwen, 2003). In this way, we allow neurons coding for the shared feature to participate to different representations during the same retrieval, avoiding a population explosion. This flexibility is not possible with coding mechanisms based on the firing rate information, due to its *transitive* character allowing also the association between neurons coding for different patterns ("ghost memories"). A *nontransitive* mechanism could be obtained through a dynamic synchrony, implementing either periodic or chaotic dynamics (see Fig. 1). However, the periodic case seems less plausible in terms of physiological evidences. As a fact, chaotic dynamics evolves over an information-loss time corresponding to the reciprocal of the positive Lyapunov exponent (roughly equal to the spike separation, that is, a few milliseconds). The onset of a synchronized state occurs within that time, whereas in a periodic dynamics there are infinitely many returns, thus, it is time consuming.

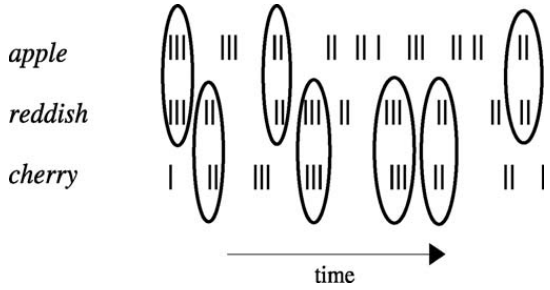

Fig. 1. An example of *nontransitive* associative mechanism of *reddish* to *apple* or *cherry*, in terms of chaotic trains of spikes.

3. The network model

We implement a neural network characterized by the *multimodular architecture* depicted in Fig. 2. It is given by a set of *M feature modules*, each representing a specific dimension, or domain, in the memory pattern (e.g. color, dimension, shape, etc.). Each module includes *F* neurons coding for different *features* of the pattern, along the dimension specified by the module (e.g. red in color module, sphere in shape module, etc.). A memory pattern is defined by a vector of *M* features, each one from a different module. In order to obtain all possible patterns, every neuron is connected via excitatory coupling to all neurons of the other modules (*cooperation* between modules). Since neurons belonging to the same module code for mutually exclusive features (e.g. either red or yellow), we also introduce a *competitive* mechanism between them. We use Hindmarsh–Rose model-neurons (HR) (Hindmarsh and Rose, 1984), which exhibit realistic response properties. Those models are characterized by a periodic or chaotic (irregular inter-spike intervals) dynamic behavior, depending on a single parameter. The

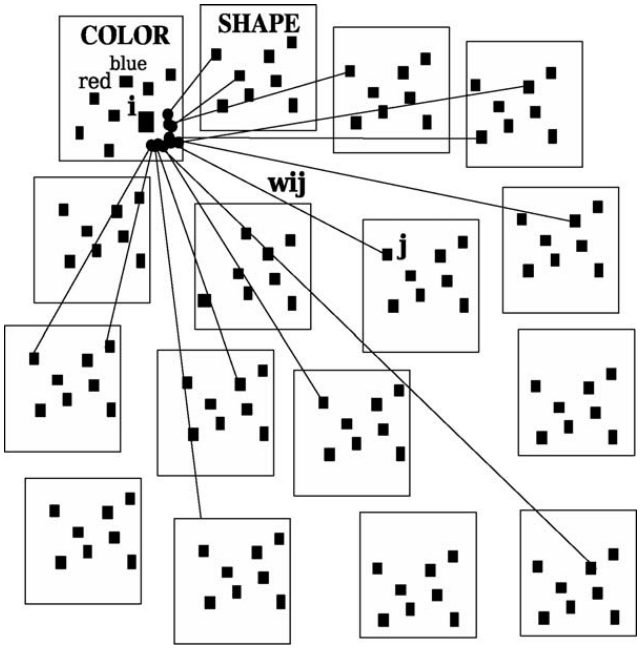

Fig. 2. Representation of the multimodular architecture. The network includes M ($M = 16$) feature modules, represented here as boxes. Each module contains F ($F = 8$) neurons, depicted as squares. Each single neuron i is connected to all neurons j in the other modules, through excitatory coupling (w_{ij}).

network consists of N HR ($N = 128$ all in the simulation here reported), belonging to M different modules ($M = 16$). In each module we have F feature neurons ($F = 8$). The single HR neuron in the network is described by the first-order differential equations:

$$\dot{X}_i = Y_i - aX_i^3 + bX_i^2 - Z_i + I_i + \alpha \sum_{j=1}^{F(M-1)} w_{ij} S_j(t) - \beta \frac{1}{F} \sum_{k=1}^{F-1} S_k^{(i)}(t) \quad (1)$$

$$\dot{Y}_i = c - dX_i^2 - Y_i \quad (2)$$

$$\dot{Z}_i = r[s(X_i - x_0) - Z_i] \quad (3)$$

In these equations, i is the index for neurons in the network, j is the index identifying neurons belonging to different modules from the module of i, k identifies neurons inside the same module as i. The state of neuron i is described by three variables, namely, the membrane potential X_i, the recovery variable Y_i, and a slow adaptation current Z_i. The external input I_i, for the standard choice of parameters ($a = 1.0$, $b = 3.0$, $c = 1.0$, $d = 5.0$, $s = 4.0$, $r = 0.006$, and $x_0 = -1.6$), is set such that the single neuron dynamics is chaotic. The synaptic input given by the firing activity of the j-th neuron on the i-th neuron is modeled in Eq. (1), by the impulse current to the i-th neuron, proportional to the synaptic strength w_{ij}, generated when the j-th neuron is active. A neuron is here considered active whenever its membrane potential exceeds a threshold value X^* ($X^* = 0$ in our study), and its activity is coded by the activity variable S_j by $S_j = \theta(X_j(t) - X^*)$, where θ is the Heaviside step function, equal to 0 for negative argument and 1 otherwise. A local inhibition mechanism, active on the i-th neuron, is modeled in Eq. (1) by a negative impulse current to the i-th neuron, generated when the k-th neuron, belonging to the same module as i, is active. Here, S_k^i, coded also by the Heaviside function, represents the activity variables of the neurons in the same module of i. The synaptic input and the local inhibition are weighted by the terms α and β, respectively. The physical time scale is not assigned in the HR dimensionless model; it is fixed by comparing the model solutions to physiological activity. The numerical integration was performed by using a fixed-step fourth-order Runge–Kutta method. The integration step-size was chosen equal to 0.05 ms to fit real data.

In order to characterize the dynamical behavior of the variable X, the time intervals between successive crossing of a threshold *thr* are recorded (*thr* is chosen greater than X^* in order to discard the near-threshold dynamics from the spiking analysis). We define the T_n time of the n-th crossing as $dX(T_n)/dt > 0$ (positive slope). The inter spike interval (ISI) is defined as $\mathrm{ISI}_n = T_{n+1} - T_n$. From the analysis of the single HR model, it is known that different qualitative behaviors, e.g. *spiking* and *bursting* dynamics, can be obtained by varying the input current I and evidenced by the ISI distributions. In Fig. 3, two different dynamics are exhibited for different values of the coupling α. For $\alpha = 0.25$ (left) a bursting dynamics (see the inset) results in a bimodal ISI distribution. The first peak corresponds to the short intervals between spikes (≈ 6 ms), the other to intervals between bursts (≈ 75 ms). For $\alpha = 0.5$ (right side), the separation between the two time scales disappears: the distribution shows only one peak around 5 ms and decays almost exponentially. The most probable ISI value (ISI^*) gives an important time scale of the system, associated with a preferred firing rate ($\mathrm{ISI}^* = 6$ ms for $\alpha = 0.25$ and 4.5 ms for $\alpha = 0.5$). The corresponding spiking dynamics is plotted in the inset. In the following, we will consider these two α values for our analysis. Just a critical comment on our choice of α. For low α values, the spikes are well segregated in bursts (sequences of spikes separated by a long inter-burst interval). As α increases, this separation reduces and eventually the inter-burst's temporal scale is not easily distinguishable from ISI's one, obtaining a spiking dynamics (Morelli, 2006). The transition from bursting to spiking dynamics is gradual. We decide

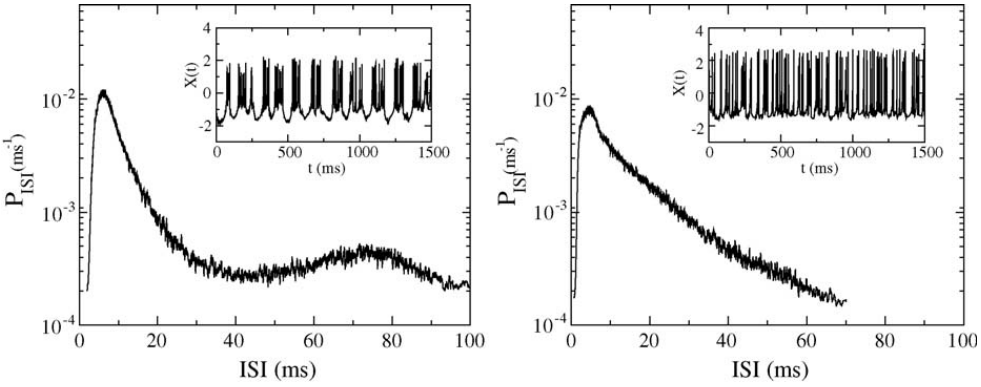

Fig. 3. ISI distributions for a single neuron, in the case of $\alpha = 0.25$ (left) and $\alpha = 0.5$ (right). In the insets, the temporal dynamics of the relative membrane potential variables are plotted.

to consider parameter values in a range which results in a plausible temporal dynamics (i.e. comparable with experimental evidences).

4. Memory patterns

Memory patterns are defined by sets of M features, coded by M active neurons, each one from a different module. Given two memory patterns, we distinguish between *patterns which do not share features* (NSF) and *patterns which share features* (SF). In the first case, vectors coding for the two patterns are orthogonal, i.e., they do not share any feature. In this case, all active neurons are coding for a pattern only. In the second case, vectors are not orthogonal, thus, some neurons are coding for more than one pattern.

5. Learning rule

We implement a *learning stage*, during which input memory patterns are stored, and a *retrieval stage*, in which the network activates some memory patterns out of the stored ones. A variable number of memory patterns is randomly generated and stored in long-term memory via updating of connection weights by a Hebbian mechanism: if two connected neurons i and j (belonging to different modules) code for a same pattern, the synaptic efficacy of their connection (w_{ij}) is increased. In this work w_{ij} is defined as

$$w_{ij} = \frac{1}{M}\frac{1}{F}\left(1 - \exp\left(-\sum_{p=1}^{P} S_i(p)S_j(p)\right)\right) \qquad (4)$$

where $S_l(p) = 1$ if neuron l is active for pattern p, $S_l(p) = 0$ otherwise; P is the number of stored patterns. The learned connection weights are kept constant during memory retrieval and successive simulations. In the next section, we report results concerning the multiple retrieval dynamics of the network. We are interested on the retrieval of patterns which share features or not.

6. Retrieval dynamics

In order to investigate the retrieval dynamics of the network, we study the temporal firing state of the neurons which are activated by input patterns (working-memory, Baddeley, 1992). We activate those neurons coding for the M features of a given pattern, by setting their external input current I_i in a chaotic regime, randomly between 3.0 and 3.1 (I_i is equal to 0 for inactive neurons). We are interested on what happens when the retrieved patterns are more than one, and when they share some features (SF) or not (NSF). Simulations were performed with a variable number of stored patterns, retrieved patterns and shared features. Here, for the sake of simplicity, we report the results concerning two simulation conditions: the retrieval of two NSF patterns, and the retrieval of two SF patterns with three shared features. In both conditions the number of stored patterns P is equal to 15. First of all, to characterize the state of synchronization between and within active memory patterns, we perform the correlation analysis between time series of active neurons. By focusing on the information carried out only by spikes, we investigate the retrieval process by looking at the state of the neurons, between and within active memory patterns, in term of their rate of coincident spikes. Then, we introduce the finite-time analysis with the aim to investigate the neural dynamics on a more appropriate time scale for the cognitive domain.

6.1. Retrieval dynamics: analysis over "long" time series

In order to characterize the degree of synchronization within and between patterns, we analyze (normalized)

correlation functions between time series $x(t)$, $y(t)$ generated by the membrane potential of the active neurons (variable X in Eq. (1)). The same analysis is performed also using binarized time series of the membrane potential, by defining a threshold in order to encode the membrane potential $X(t)$ of the neurons as a string of 0s and 1s. The latter analysis aims to determine if the binary format can encode the same information, i.e. if this information is sufficient to describe the correlation structure of the retrieved patterns. Since the temporal data about the spikes (their temporal position, length and separation from other spikes) are maintained in binarized time series, we expected that they represent the main source of information in the signal and therefore the structure does not change dramatically for the binarized time series. Given the spiking nature of our dynamics, we also introduce the *coincidence analysis*, which could better describe the spiking behavior of the system. This latter analysis has been widely used in the literature on neural coding (see, for example, Quiroga et al., 2002; Hahnloser et al., 2002). As in the case of correlation analysis with binarized time series, the sub-threshold component and the signal shape are ruled out. Here, the basic assumption is that the information is carried out by the spikes, and that the segregation of the spike trains between and within active memory patterns could be made in terms of coincident spikes. The coincidence rate indicator (Cr) is defined as the rate of coincidences between two binarized time series $X(t)$ and $Y(t)$, normalized to the individual spiking rates. Our 'coincident events' are obtained from $XY(t) = X(t)$ AND $Y(t)$. Cr is defined as

$$\mathrm{Cr} = \frac{N_{XY}}{\sqrt{N_X N_Y}} \tag{5}$$

where N_X is the number of spikes in $X(t)$, and N_Y in $Y(t)$, and N_{XY} is the number of coincident events. The three indicators are used in the following retrieval conditions.

Retrieval of patterns with not shared features (NSF). We activate two NSF patterns (Pattern I and Pattern II) out of the P stored patterns. We have a total of 32 active neurons, each coding for one pattern only. By analyzing the structure of correlation functions for the full signal shape and binarized time series, we find stronger correlations between neurons coding for the same pattern, and weaker correlations between neurons coding for different patterns (Fig. 4, left side and center, respectively). The same results are obtained evaluating the coincidence rates (Fig. 4, right side). The structure of the matrices is the same for the three different analyses.

Retrieval of patterns with shared features (SF). In this second condition, the network retrieves two SF patterns which share three features (three neurons are coding for both Pattern I and Pattern II). By evaluating the values of the correlation functions for the normal and binarized time series (Fig. 5, left side and center, respectively), we observe stronger correlations between neurons coding for the same pattern and weaker correlations between neurons coding for different patterns, except for those neurons coding for shared features: they are correlated with neurons coding for both Pattern I and Pattern II. The same results are obtained evaluating the coincidence rates. As in the NSF condition, the structure of the matrices is the same.

6.2. Retrieval dynamics: "finite-time" analysis

Long time series analysis have been performed on series longer than 10,000 ms, necessary for the statistical convergence of the indicators. On the other hand, since a categorization task (e.g. visual categorization of a natural scene) takes about 100 ms, is it natural to wonder if the

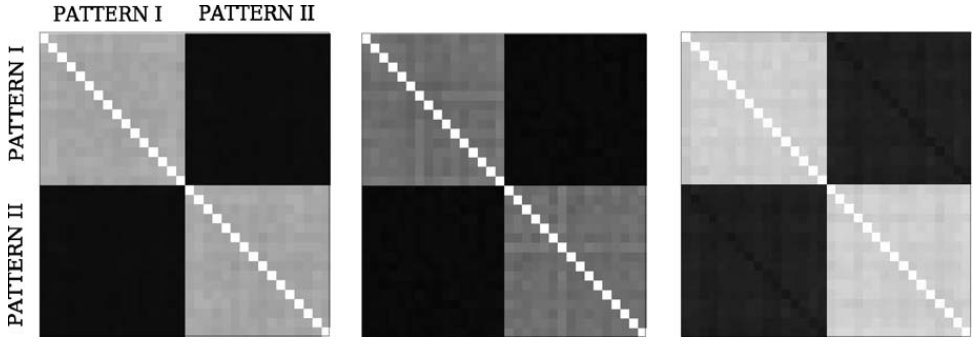

Fig. 4. Retrieval of two patterns with not shared features. Correlation and coincidence values are evaluated between time series of the membrane potential of active neurons (16 for Pattern I and 16 for Pattern II). Left: correlation values; center: correlation values obtained with binarized time series; right: coincidence rate values; within each matrix: the correlation and coincidence values for the 16 pairs of neurons belonging to Pattern I and Pattern I (top-left), Pattern I and Pattern II (top-right), Pattern II and Pattern I (bottom-left), Pattern II and Pattern II (bottom-right). Values are represented using grayscales, from 0 (black) to 1 (white), obtained for $\alpha = 0.5$. The threshold for binarization is chosen equal to 0.75.

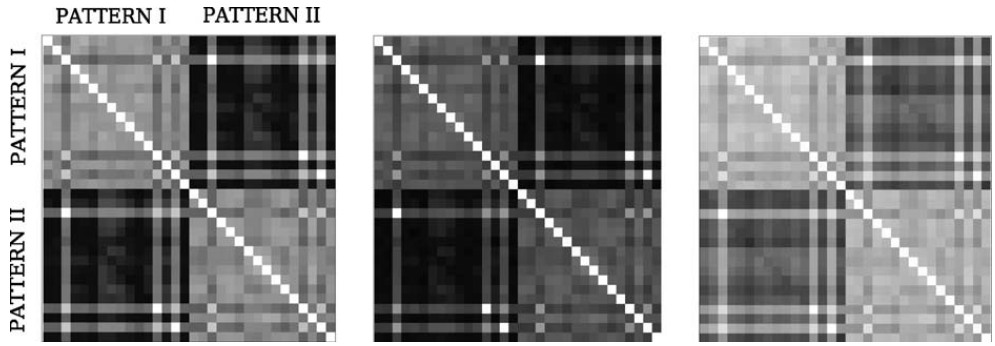

Fig. 5. Retrieval of two patterns with three shared features. Correlation and coincidence values are evaluated between time series of the membrane potential of active neurons (13 for Pattern I only, 13 for Pattern II only, and 3 for both). Left: correlation values; center: correlation values obtained with binarized time series; right: coincidence rate values. The structure of the matrices is the same as in Fig. 4.

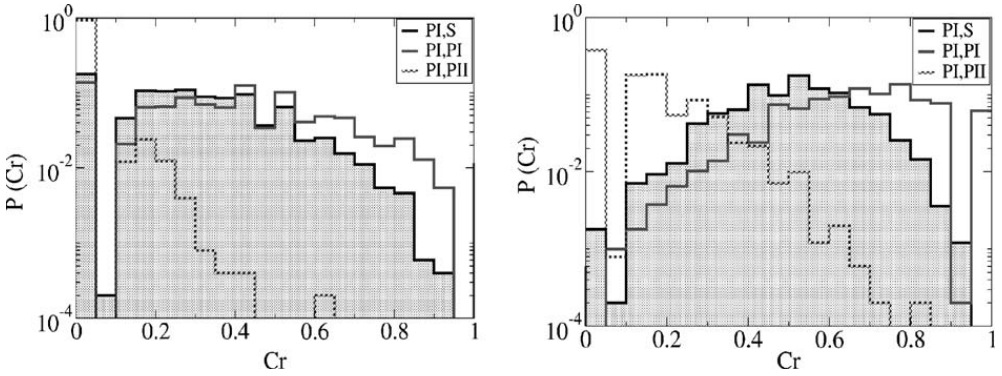

Fig. 6. Distributions of Cr in the SF condition, obtained from three couples of active neurons (see text). The distributions are evaluated for $\alpha = 0.25$ (left) and $\alpha = 0.5$ (right).

time scale of the correlation analysis is plausible from a cognitive point of view. In other words, we ask ourself if a comparable amount of information, obtained from the analysis of long time series, can be inferred from finite temporal windows. In order to investigate this possibility, the first problem concerns the choice of the window length. Electrophysiological data, obtained by using an alternating dual-task event-related potential (ERP) experimental paradigm, showed that visual categorization of a natural scene could be performed above chance in less than 250 ms (Van Rullen and Thorpe, 2001). This surprisingly short value gives roughly an approximation of the category process duration. Other results on complex scenes categorization show similar short intervals (about 150 ms) (Antal et al., 2002). Following these indications, we therefore investigate if the information contained in "finite-time" windows of such a short duration could be enough for the association of the firing activities to the right memory patterns. We start our analysis by choosing a window length of 100 ms. Using this length, we perform the correlation and coincidence analysis (defined in Section 6.1) on finite-time windows. The following analysis is performed in the more relevant case of the SF condition. As preliminary analysis, we reproduce the same pattern results obtained for long time series (plotted in Fig. 5), by evaluating the correlation and coincidence indicators over independent finite-time windows (Morelli, 2006).

Here, we consider only those windows where at least one neuron is firing; we call them *significant events* (SE's). This criterion is used here to distinguish in the case of $Cr = 0$ when there is no spike coincidence, from when a coincidence/no coincidence decision could not be taken because both neurons are silent. In Fig. 6, we plot the Cr distributions in the cases of three pairs of neurons (i, j), namely, (i, j) coding for different patterns (PI, PII), (i, j) coding for the same pattern (PI, PI), and i coding for Pattern I and j is the shared (S) neuron coding for both Patterns I and II (PI, S)[1]. We find that the three cases are statistically distinguishable for the coupling $\alpha = 0.5$. In this case, neurons coding for the same pattern show an asymmetric distribution towards 1, indicating a high rate of coincidences. Vice versa, the Cr

[1] The corresponding pair (PII, S) has been also evaluated. Since the same results are obtained, for the sake of simplicity we present here only the pair (PI, S).

distribution for neurons of different patterns is asymmetric towards zero. The distribution related to the shared neuron is peaked around 0.5, and it is symmetric. These results are consistent with our expectations of finding a low coincidence probability between neurons coding for different patterns, high probability for neurons of the same pattern, and an intermediate value for the shared neuron, likely correlated with neurons coding one pattern only. For $\alpha = 0.25$, the distributions are less separated and shifted towards zero.

Similar results, indicating an intermediate condition for shared features between neurons coding for one pattern only, have been obtained in our previous study (Morelli et al., 2005). There, we have analyzed the indicator values for running time windows, in order to investigate the temporal alternation in the synchronization between the shared neuron and the other neurons coding for a pattern only. We expected simultaneous high-low values in the (PI, S)–(PII, S) pair, and the alternation with (PII, S) high–(PI, S) low of this situation as suggestive of the alternating synchronization of the shared neuron. The data indicated the presence of this effect, but they also suggested that suitable criteria concerning the quality of temporal separation were needed. For example, the definition of a *criteria for pattern inclusion* (how much neuron S is correlated with PI or PII), and a *criteria for pattern separation* (e.g. a simultaneous high correlation of neuron S with PI and a low correlation with PII), are necessary. The problem implies some hypothesis on a possible readout mechanism of neural coding. We introduce some indicators which could be used in the readout.

First, we define the joint probability density $Q(x, y)$ of coincidence value x for (PI, S) and y for (PII, S). Q is evaluated only over couples of SE's; in this case, we generalize a significant event by considering only those windows where in both couples of neurons at least one is firing, as we are interested in the *simultaneous* activity. We point out also that the statistics of the SE's is an important measure of the efficiency of a readout mechanism based on Q, and it could be useful to identify a time scale of coding/decoding. For this purpose, we report in Fig. 7 the probability PSE of SE's versus the windows length. PSE increases with the window length, saturating at 1 for about 50 ms for $\alpha = 0.5$ (dashed line), and 70 ms for $\alpha = 0.25$ (continuous line). This effect can be understood with the help of the ISI distributions. For windows shorter than ISI*, the PSE is low because of the low probability to have a spike in the intervals. As the window duration increases, becoming comparable to, or greater than, ISI*, the contributions related to the presence of more spikes became relevant. The difference of PSE for $\alpha = 0.25$ and 0.5 can be thus related to the

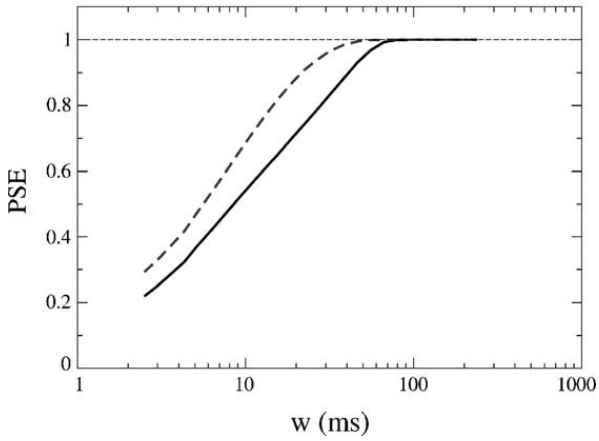

Fig. 7. Probability of couples of significant events, evaluated for $\alpha = 0.25$ (full line) and $\alpha = 0.5$ (dashed line).

difference between the ISI distributions in the two cases. Since for the same window length it is more probable to find a higher number of spikes for $\alpha = 0.5$ than for $\alpha = 0.25$, it is plausible to obtain a comparably higher PSE with the first case.

When the two couples of neurons are firing, the analysis of the distribution Q allows a description of the details of the simultaneous activity. In Fig. 8 we plot the $Q(x, y)$ distribution evaluated for $\alpha = 0.25$ (top) and $\alpha = 0.5$ (bottom), by using finite-time windows of length $w = 10$ ms (left) and $w = 100$ ms (right). For both α values, in the case of $w = 10$ms, Q takes a restricted number of values, mostly near to the axes and in a regular grid. Such a discrete structure reflects the separation between different values of the Cr indicator for such a short time window. Indeed, when a fluctuation of the value is realized due to a neuron firing/not firing in the window, the effect is comparably higher than in longer windows. For $w = 100$ ms the probability density spreads out; for $\alpha = 0.25$ the values close to (0,0) are more probable (in agreement with the asymmetric distribution of Fig. 6 (left)), while for $\alpha = 0.5$ the more probable values are in the center (symmetric distribution of Fig. 6 (right)); in this case, there are no or very few values on the axes, and mostly comparable values of coincidences for (PI, S) and (PII, S).

The joint probability density can be used to characterize the quality of temporal separation. We introduce a criterion in order to quantify the cases in which neuron S shows a high coincidence value with a neuron coding for PI and a low value with one coding for PII, and vice versa. This criterion relies on the estimation of the measure:

$$Q_r = \int_0^{\theta_1} dx \int_{\theta_2}^1 dy Q(x, y) + \int_0^{\theta_1} dy \int_{\theta_2}^1 dx Q(x, y) \quad (6)$$

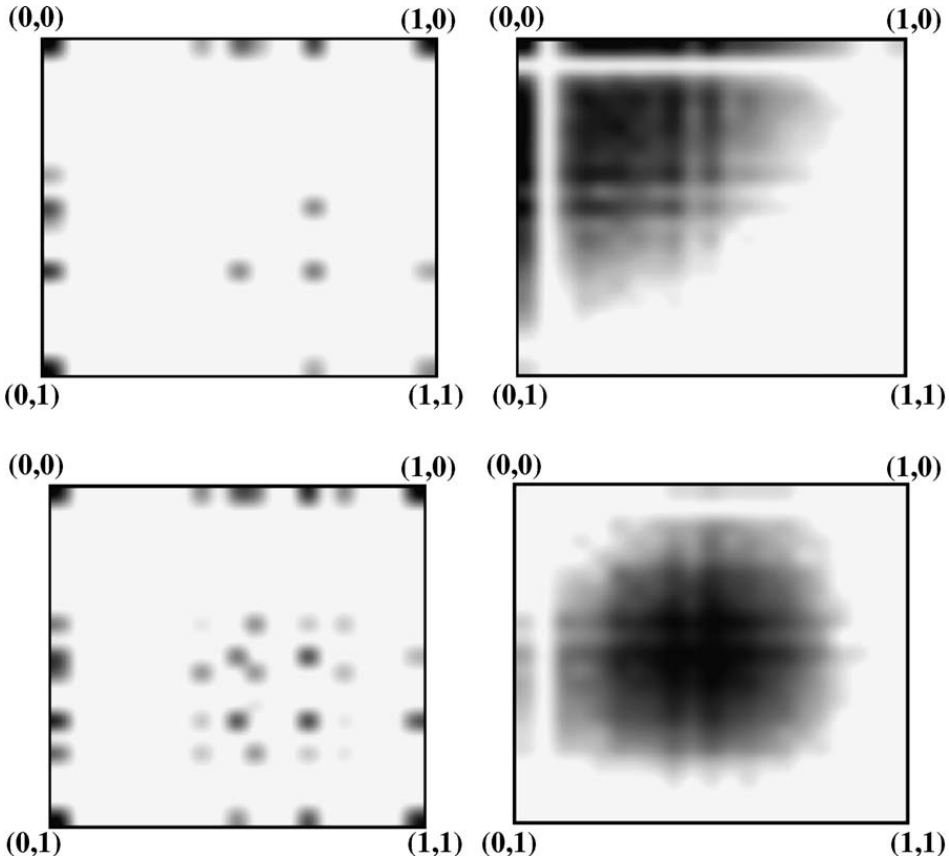

Fig. 8. Joint probability density Q, evaluated for $\alpha = 0.25$ (top) and $\alpha = 0.5$ (bottom) by using finite-time windows of length $w = 10$ ms (left) and $w = 100$ ms (right). Values are represented using grayscales, from 0 (white) to 1 (black).

where θ_1 and θ_2 are the confidence thresholds for the temporal separation; in the following, we have chosen $\theta_1 = \theta_2 = 0.5$. The indicator Q_r represents the probability of the events $(0 < x < \theta_1, \theta_2 < y < 1)$, i.e., shared neuron "far" from (not coding for) PI and "close" to (coding for) PII, or $(\theta_2 < x < 1, 0 < y < \theta_1)$, i.e., shared neuron "close" to (coding for) PI and "far" from (not coding for) PII. Our criterion is satisfied when the indicator approaches 1, implying an high probability to have an unambiguous coding of neuron S. The indicator is evaluated for different window lengths (from 2.5 to 240 ms) and plotted in Fig. 9. A maximum is present in the probability curves, corresponding to optimal window lengths. For $\alpha = 0.25$ the probability display a maximum around 13 ms for Q_r, while for $\alpha = 0.5$ the maximum is around 7 ms. It should be noted that such lengths are quite short (about two times the corresponding ISI*), suggesting that our indicator is maximized by coincidences carried out by two to three spikes at a time. We notice also that for $\alpha = 0.5$ Q_r remains around 0.5 at increasing window lengths, while for $\alpha = 0.25$ it approaches 0. This can be understood by looking at the shape of the Q distributions, as plotted in Fig. 8 (right) for $w = 100$ ms. Indeed, while for $\alpha = 0.5$ the density Q is homogeneously broadened around the center of the domain, leading to a value of Q_r close to 0.5, for $\alpha = 0.25$ the higher probable values of Q are asymmetrically close to (0,0), thus, resulting in a low value of Q_r. In the inset of Fig. 9 we also consider the product $\bar{Q}$ of Q_r for the corresponding PSE's, obtaining the absolute probability to satisfy our criterion, i.e., including all the possible cases of firing/not firing. Since PSE depends monotonically on the window length, the absolute probability displays a shifted position of the maxima towards longer durations, keeping however the structure of Q_r. A remarkable difference is present in the case of $\alpha = 0.5$, where the maximum is replaced by a saturation behavior for windows longer than about 20 ms. For $\alpha = 0.25$ the maximum is shifted around 36 ms. The evaluation of Q_r for windows of length comparable to cognitive decision times (around 150 ms) shows that the higher value is reached for $\alpha = 0.5$ than for $\alpha = 0.25$. This seems to suggest that a spiking dynamics could favor a less ambiguous coding of the shared neuron. We point out that the maxima reached by the indicator in the two cases show that a better coding can be obtained for time scales much shorter than 100 ms, just by using two to three spikes. We now formulate a general conjecture on how a cognitive agent goes beyond the

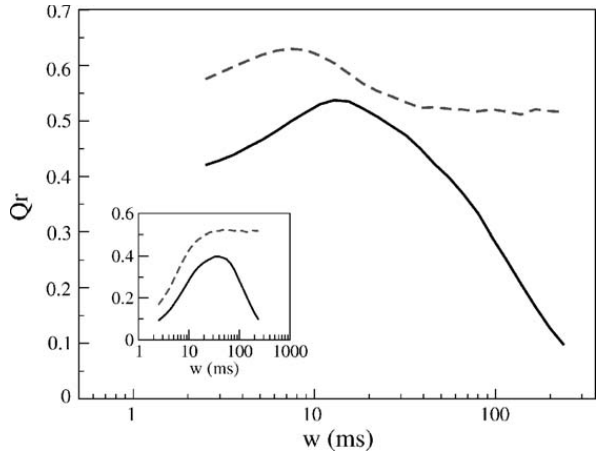

Fig. 9. Q_r probability for $\alpha = 0.25$ (continuous) and $\alpha = 0.5$ (dashed). In the inset we plot the product of Q_r with the SE probability.

computational paradigm. In a real brain, structured over several hierarchical levels, a cognitive sub-system as the one sketched in Fig. 2 will be followed by a decisional system (DS). Based on the global information available in the dynamical system of Fig. 2, DS will activate some efferent channels (e.g. specific motor neurons). It is a plausible guess to expect that DS does not act upon the point-to-point information of Fig. 2 (in such a case there would be no reason to have a DS operationally separated) but upon some collective indicators. The inset of Fig. 9 shows that for $\alpha = 0.5$ once $\bar{Q}$ reaches its asymptotic value (in about 10 ms) it can be used as a holistic indicator.

7. Conclusions

The investigation of the retrieval dynamics of multiple memory patterns is performed by characterizing the neuronal activity within and between active memory patterns. By using the correlation and coincidence analysis over long time series, it is possible to identify for which pattern the neurons are coding for, in the case of overlapping and non-overlapping patterns. In the more relevant case of overlapping patterns (SF condition), a study over finite-time windows is introduced. This is supported by experimental evidence showing the capability of human neural processes in making a decision in a relatively short time interval. The finite-time analysis is thus performed by using coincidence analysis over cognitively relevant time windows. A statistical analysis of the indicator show similar results of those obtained evaluating long time series. The joint probability analysis is thus applied in order to investigate the behavior of shared neurons, which are coding for more than one active memory patterns. This analysis indicates that a short time scale (corresponding to about two to three spikes) could be sufficient to perform the coding of the shared neurons, provided that conditions of minimal activity are fulfilled. Moreover, in the case of spiking dynamics the coding could be operated also using temporal windows of lengths comparable with cognitive decision times. The quality of the indicators described here is strongly related to the choice of readout mechanism used to decode the neuronal activity. This problem is not simply a technical matter, but it requires further investigation.

Acknowledgments

We are grateful to G. Giacomelli and T. Kreuz for helpful discussions. This work was partially supported by Ente Cassa di Risparmio di Firenze under the Project “Dinamiche cerebrali caotiche” and by the EU under the ENOC COST action B27.

References

Amit, D., 1998. Modeling Brain Function. Cambridge University Press, Cambridge, UK.

Antal, A., Keri, S., Kincses, T., Kalman, J., Dibo, G., Benedek, G., Janka, Z., Vecsei, L., 2002. Corticostriatal circuitry mediates fast-track visual categorization. Cogn. Brain Res. 13, 53–59.

Baddeley, A.D., 1992. Working memory. Science 255, 556–559.

Bussey, T.J., Saksida, L.M., Murray, E.A., 2003. Impairments in visual discrimination after perirhinal cortex lesions: testing ‘declarative’ vs ‘perceptual-mnemonic’ views of perirhinal cortex function. Eur. J. Neurosci. 17, 649–660.

Engel, A.K., König, P., Kreiter, A.K., Schillen, T.B., Singer, W., 1992. Temporal coding in the visual cortex: new vistas on integration in the nervous system. Trends Neurosci. 15, 218–226.

Gray, C.M., 1999. The temporal correlation hypothesis of visual feature integration: still alive and well. Neuron 24, 31–47.

Hahnloser, R.H.R., Kozhevnikov, A.A., Fee, M.S., 2002. An ultra-sparse code underlies the generation of neural sequences in a songbird. Nature 419, 65–70.

Hindmarsh, J.L., Rose, R.M., 1984. A model of neuronal bursting using three coupled first order differential equations. Proc. R. Soc. Lond. B: Biol. Sci. 221, 87–102.

Morelli, A., 2006. A feature-based semantic memory model: retrieval dynamics of multiple memory patterns. PhD dissertation, University of Florence, Italy.

Morelli, A., Lauro Grotto, R., Arecchi F.T., 2005. A feature-based model of semantic memory: the importance of being chaotic. In: De Gregorio, M., Di Maio, V., Frucci, M., Musio, C. (Eds.), Brain, Vision, and Artificial Intelligence. Lecture Notes in Computer Science. Springer-Verlag, Berlin, Heidelberg, pp. 328–337.

Plaut, D., 1995. Semantic and associative priming in a distributed attractor network. In: Moore, J.D., Lehman, J.F. (Eds.), Proceedings of the 17th Annual Conference of the Cognitive Science Society, Lawrence Erlbaum Associates, Hillsdale, pp. 37–42.

Quiroga, R.Q., Kreuz, T., Grassberger, P., 2002. Event synchronization: simple and fast method to measure synchronicity and time delay patterns. Phys. Rev. E 66, 041904–041913.

Raffone, A., Van Leeuwen, C., 2003. Dynamic synchronization and chaos in associative neural network with multiple active memories. Chaos 13, 1090–1104.

Rumelhart, D.E., 1990. Brain style computation: learning and generalization. In: Zornetzer, S.F., Davis, J.L., Lau, C. (Eds.), An Introduction to Neural and Electronic Networks. Academic Press, San Diego, pp. 405–420.

Segev, R., Benveniste, M., Hulata, E., Cohen, N., Palevski, A., Kapon, E., Shapira, Y., Ben-Jacob, E., 2002. Long term behavior of lithographically prepared in vitro neuronal networks. Phys. Rev. Lett. 88, 1181021–1181024.

Shallice, T., 2002. Fractionation of the supervisory system. In: Stuss, T.S., Knight, R. (Eds.), Principles of Frontal Lobe Function. Oxford University Press, Oxford, UK, pp. 261–277.

Treves, A., 2005. Frontal latching networks: a possible neural basis for infinite recursion. Cogn. Neuropsychol. 22, 276–291.

Van Rullen, R., Thorpe, S., 2001. The time course of visual processing: from early perception to decision-making. J. Cogn. Neurosci. 13, 454–461.

Von der Malsburg, C., 1999. The what and why of binding: the modeler's perspective. Neuron 24, 95–104.